

FFI RAPPORT

PENETRATION MODELLING WITH UNCERTAINTY QUANTIFICATION USING THE WALKER-ANDERSON MODEL

SOLENG Harald H, SVINSÅS Eirik

FFI/RAPPORT-2000/05876

FFIBM/766/130

Approved
Kjeller 15 January 2001



Bjarne Haugstad
Director of Research

**PENETRATION MODELLING WITH
UNCERTAINTY QUANTIFICATION USING THE
WALKER-ANDERSON MODEL**

SOLENG Harald H, SVINSÅS Eirik

FFI/RAPPORT-2000/05876

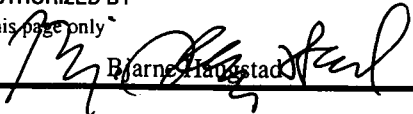
FORSVARETS FORSKNINGSINSTITUTT
Norwegian Defence Research Establishment
P O Box 25, NO-2027 Kjeller, Norway

FORSVARETS FORSKNINGSPINSTITUTT (FFI)
Norwegian Defence Research Establishment

UNCLASSIFIED

P O BOX 25
NO-2027 KJELLER, NORWAY
REPORT DOCUMENTATION PAGE

SECURITY CLASSIFICATION OF THIS PAGE
(when data entered)

1) PUBL/REPORT NUMBER FFI/RAPPORT-2000/05876	2) SECURITY CLASSIFICATION UNCLASSIFIED	3) NUMBER OF PAGES 21
1a) PROJECT REFERENCE FFIBM/766/ 130	2a) DECLASSIFICATION/DOWNGRADING SCHEDULE -	
4) TITLE PENETRATION MODELLING WITH UNCERTAINTY QUANTIFICATION USING THE WALKER-ANDERSON MODEL		
5) NAMES OF AUTHOR(S) IN FULL (surname first) SOLENG Harald H, SVINSÅS Eirik		
6) DISTRIBUTION STATEMENT Approved for public release. Distribution unlimited. (Offentlig tilgjengelig)		
7) INDEXING TERMS IN ENGLISH:		
IN NORWEGIAN:		
a) <u>Penetration</u>	a) <u>Penetrasjon</u>	
b) <u>Uncertainty</u>	b) <u>Usikkerhet</u>	
c) <u>Concrete</u>	c) <u>Betong</u>	
d) _____	d) _____	
e) _____	e) _____	
THESAURUS REFERENCE:		
8) ABSTRACT We perform a detailed critical study of the Walker–Anderson analytical penetration model. It is shown that the velocity profile assumed by Walker and Anderson has a discontinuity in its first derivative at the elastic-plastic boundary. Fortunately, for our test data set, this somewhat unphysical feature is shown to be benign and practically unimportant. Then the Walker–Anderson model is compared with a rigid penetration model and as expected, the effects of projectile deformation and erosion are found to be very important. Finally we perform a statistical analysis of the Walker–Anderson model applied to penetration of concrete with uncertain target data.		
9) DATE 15 January 2001	AUTHORIZED BY This page only  Bjarne Haugstad	POSITION Director of Research

ISBN 82-464-0491-1

UNCLASSIFIED

SECURITY CLASSIFICATION OF THIS PAGE
(when data entered)

CONTENTS

	Page	
1	INTRODUCTION	7
2	FORMULATION OF THE MODEL	8
2.1	Conservation of momentum	9
2.2	Velocity profile	10
2.3	Continuity of u_z over projectile–target interface	10
2.4	Stress behaviour in the target	11
2.5	Deceleration of the tail	11
2.6	Equations of motion	12
3	APPLICATION TO CONCRETE PENETRATION	13
3.1	Model breakdown	13
3.2	Results of numerical integration	13
3.2.1	Effect of smoothed velocity profile	13
3.2.2	Comparison with rigid penetration	15
3.2.3	Prediction uncertainties from parameter uncertainties	15
4	CONCLUSION	16
APPENDIX		
A	NOTATION	18
	References	19
	Distribution list	21

PENETRATION MODELLING WITH UNCERTAINTY QUANTIFICATION USING THE WALKER-ANDERSON MODEL

1 INTRODUCTION

In the field of penetration mechanics, several different analytical models are available. Depending on the impact velocity and the material properties of the projectile and target, the projectile may be described as a rigid body, as an elastic-plastic eroding body, or by the laws of hydrodynamic flow alone. The first case is e.g. relevant in cases where a conventional shell or missile penetrates a soft target of soil or normal concrete, while the latter is suited for describing shaped charge penetration. The eroding body formulation will in most cases be necessary when treating modern high velocity sub-calibre ammunition.

Of the three classes above, the elastic-plastic eroding body models are the most involved, as the elastic-plastic material properties of both projectile and target must be considered on a physically sound basis. We may here extend the meaning of “plasticity” to include irreversible deformations of brittle materials as a result of internal microcracking. The earlier models [1, 2, 3] known from the literature¹, are mostly extensions of the first hydrodynamic approaches by Birkhoff et al. [5], with the aim of including the deceleration of the body together with the rigid-penetrator behaviour during the last phase.

The model of Walker and Anderson [6, 7] is one of the most advanced so far. It makes use of centerline momentum balance together with assumed velocity fields, and has been shown to yield good results for penetration of metals and ceramics. In this report, we investigate the application of the model to concrete and rock targets with uncertainties in the material data.

In doing so, we start out with a short review in Chapter 2 and point out a discontinuity in the first derivative of the velocity field over the elastic-plastic boundary in the projectile. A generalization without this unwanted feature is then proposed.

In Chapter 3, a generic concrete is defined and numerical integration of the equations is performed. It is found that the generalization described earlier has very little effect, and we therefore return to the original Walker-Anderson model. It turns out that the transition to rigid-body motion is not handled well for this data set, and a rigid penetration model is therefore introduced “manually”. On comparing with predictions from a simple rigid penetration model we find, as expected, a large difference in the results.

Finally, the Walker-Anderson model is applied to penetration of concrete targets with uncertainties in the material data and a statistical analysis is performed. This approach allows us to predict penetration depth and residual mass of the projectile with quantified uncertainties in the final answers, an approach rarely seen within this field, and hardly obtainable when using numerical tools like hydrocodes. Nevertheless, a mathematically sound treatment of the uncertainties is very important. Assume that you are sitting in a bunker. Your shield is threatened by a particular weapon at a given distance. The numerical simulation tool tells you that the penetration depth of this particular weapon would be 54 cm into your protective shield. Would you feel safe behind your 60 cm walls?

¹For a recent review of analytical penetration mechanics see Ref. [4]

Neglecting the possibility of repeated hits, it would of course depend on the uncertainty of the model's prediction of a 54 cm penetration depth.

The numerical computations needed to carry out an integration of the Walker–Anderson model are many orders of magnitude smaller than that of a full-fledged hydrocode simulation. Therefore we can afford to vary the model parameters within their uncertainties and perform thousands of integrations of the model so as to span the uncertainty space and give a reliable quantification of the uncertainty of the prediction. If a trusted model predicted a (54 ± 10) cm penetration depth, then I guess you would escape the bunker!

The last Chapter 4 contains a short discussion of the results and concluding remarks.

2 FORMULATION OF THE MODEL

The Walker–Anderson model addresses the problem of a projectile hitting a homogeneous and isotropic target orthogonally to the impact surface. With these symmetry assumption the problem is axisymmetric and thus essentially two-dimensional. With simplifying assumptions it is possible to integrate out both the radial and axial dimension, and hence the problem is reduced to a set of coupled equations for two point particles representing the projectile nose and tail.

Due to different nose and tail velocities implied by the model the penetrator deforms and erode during penetration. Thus the Walker–Anderson model should be used only for penetration with eroding projectiles.

In this section we review the derivation of the Walker–Anderson model.

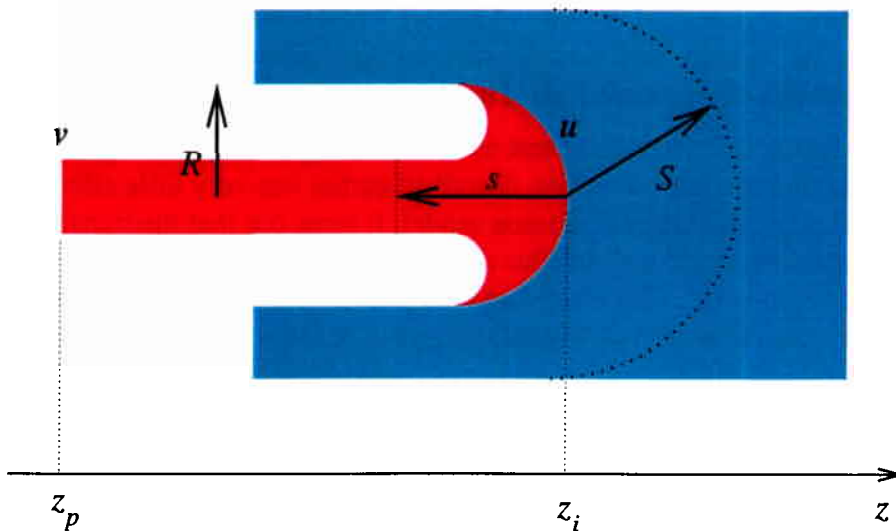


Figure 2.1: Schematic snapshot of the penetration. The nose and tail velocities are denoted u and v , respectively. The crater radius R , the radius of plasticity S of the target, and the extent of plasticity in the projectile s are indicated.

2.1 Conservation of momentum

The situation short after impact is depicted in Fig. 2.1. Let z be the position along the axis of the projectile¹, and let time be denoted by t . Using the comma notation for partial derivatives, the z -component of the Eulerian momentum equation is

$$\rho \left(u_{z,t} + \sum_i u_i u_{z,i} \right) = \sum_i \sigma_{zi,i}, \quad (2.1)$$

where ρ , σ_{ij} , and u_k are the density, stress tensor, and velocity field, respectively.

Due to axial symmetry, the equation reduces to

$$\rho \left(u_{z,t} + \frac{1}{2} \partial_z (u_z)^2 \right) - \sigma_{zz,z} - 2\sigma_{zx,x} = 0. \quad (2.2)$$

Let us now integrate Eq. (2.2) along the axis of symmetry. Let z_p be the position of the tail of the projectile, and let z_i be the interface position. Then $u(\infty) = 0$, $u_z(z_p) = v$ and $u_z(z_i) = u$, $\sigma_{zz}(z_p) = 0$, and $\sigma_{zz}(\infty) = 0$. Assuming that the projectile density ρ_p and the target density ρ_t can be regarded as constants in the integration, we get

$$\rho_p \int_{z_p}^{z_i} u_{z,t} dz + \rho_t \int_{z_i}^{\infty} u_{z,t} dz + \frac{1}{2} \rho_p (u^2 - v^2) - \frac{1}{2} \rho_t u^2 - 2 \int_{z_p}^{\infty} \sigma_{zx,x} dz = 0. \quad (2.3)$$

To integrate further we have to specify the velocity profile u_z and the shear stress behaviour.

In numerical simulations one is able to “observe” the velocity profile inside both the target and the projectile. This information was used by Walker and Anderson [6] to write down a simple expressions for u_z . As shown in their Fig. 3 the assumed velocity profile displays a similarity to that from the numerical simulation except for a discontinuity in the first

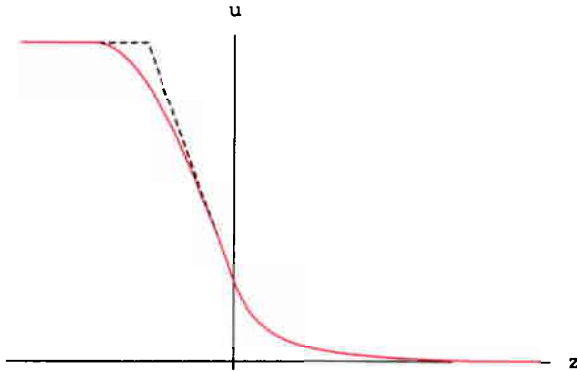


Figure 2.2: The Walker–Anderson [6] velocity profile (dashed curve) and the smoothed velocity profile derived in this report. The nose of the projectile is at the origin of the z -coordinate.

derivative at the boundary of the plastic region of the projectile. By a simple modification of the velocity profile we can remove this feature and thus make the assumed velocity profile even more similar to those of numerical simulations.

¹A complete list of symbols is given in Appendix A.

2.2 Velocity profile

Let s denote the extent of the plastic zone in the projectile and let $\varepsilon \in [0, 2)$ be a shape parametre for the velocity curve so that the velocity profile has a continuous spatial derivative along the centerline if $\varepsilon > 0$. Then we can define the centerline velocity as

$$u_z = \begin{cases} v & z_p \leq z < z_i - s \\ u + (u - v)[s(2 - \varepsilon)]^{-1} \left[2(z - z_i) + s\varepsilon \left(\frac{z - z_i}{s} \right)^{2/\varepsilon} \right] & z_i - s \leq z < z_i. \end{cases} \quad (2.4)$$

In the limit $\varepsilon \rightarrow 0$, this expression reduces to the Walker–Anderson profile, cf. Fig. 2.2. Thus, the projectile moves as a rigid object up to its plastic zone near the nose. At the boundary of the plastic zone there is a relatively sharp transition to a linearly falling velocity field. In the limit $\varepsilon \rightarrow 0$, the transition region vanishes.

Thus

$$\int_{z_p}^{z_i} u_{z,t} dz = (2 + \varepsilon)^{-1} \left[-(2 + \varepsilon)u(u - v) + (u - v)\dot{s} + s\dot{u} + ((2 + \varepsilon)L - s)\dot{v} \right] \quad (2.5)$$

where L is the length of the projectile, i.e. $L = u - v$.

Let \mathcal{R} and \mathcal{S} be the crater radius and the plasticity radius of the target. Again based on results from numerical simulations, Walker and Anderson wrote down the following expression for the centerline velocity profile of the target [6]

$$u_z = \begin{cases} u \left(\frac{\mathcal{S}^2}{(z - z_i + \mathcal{R})^2} - 1 \right) \left(\frac{\mathcal{S}^2}{\mathcal{R}^2} - 1 \right)^{-1} & z_i \leq z < z_i + \mathcal{S} - \mathcal{R} \\ 0 & z \geq z_i + \mathcal{S} - \mathcal{R}. \end{cases} \quad (2.6)$$

In the second term of Eq. (2.3), we need $u_{z,t}$ in the target. Assuming a constant crater radius \mathcal{R} , the velocity profile of Eq. (2.6) gives

$$\int_{z_i}^{\infty} u_{z,t} dz = \frac{2\mathcal{R}^2 u}{(\mathcal{R} + \mathcal{S})^2} \dot{\mathcal{S}} + \frac{\mathcal{R}(\mathcal{S} - \mathcal{R})}{\mathcal{R} + \mathcal{S}} \dot{u} + u^2. \quad (2.7)$$

2.3 Continuity of u_z over projectile–target interface

We assume that the velocity profile has a continuous derivative over the projectile–target interface

$$\left. \frac{\partial u_z}{\partial z} \right|_{z_i^-} = \left. \frac{\partial u_z}{\partial z} \right|_{z_i^+}. \quad (2.8)$$

Using Eqs. (2.4)–(2.6) and solving for s yields

$$s = \frac{\mathcal{R}(\mathcal{S}^2 - \mathcal{R}^2)(v - u)}{(2 + \varepsilon)\mathcal{S}^2 u}. \quad (2.9)$$

2.4 Stress behaviour in the target

With the assumption that the target is behaving in a perfectly plastic manner with a *constant flow stress*, and that the velocity field is tied together with the flow field for the shear stress, the last term of Eq. (2.3) evaluates to [6]

$$\int_{z_p}^{\infty} \sigma_{xz,x} dz = -\frac{7}{6} Y_t \log \frac{S}{\mathcal{R}} \quad (2.10)$$

where Y_t is the target yield limit. In the derivation of this expression it is assumed that Y_t is *constant*. However, in general the yield limit of a material varies with its state. Thus there is a mismatch between reality and the mathematical model. It can be compensated only by assigning a greater uncertainty to the yield limit or by generalizing the Walker–Anderson model so as to include a more advanced constitutive model.

2.5 Deceleration of the tail

The tail is decelerated by elastic waves. With the change in particle velocity at the free surface being twice the particle velocity of the wave,

$$\Delta v = -2c \frac{\sigma_p}{E_p} \quad (2.11)$$

during the round trip time of the wave. Here c is the speed of sound in the projectile.

The waves propagate between the elastic-plastic interface and the tail of the projectile. Consider such a wave starting from the elastic-plastic interface near the nose of the projectile at time t_i . At the time t_r the wave is reflected off the projectile tail before returning to the elastic-plastic interface at t_f . See the space-time diagram of Fig. 2.3 for a geometric picture of the world line of this wave as seen in the rest frame of the tail.

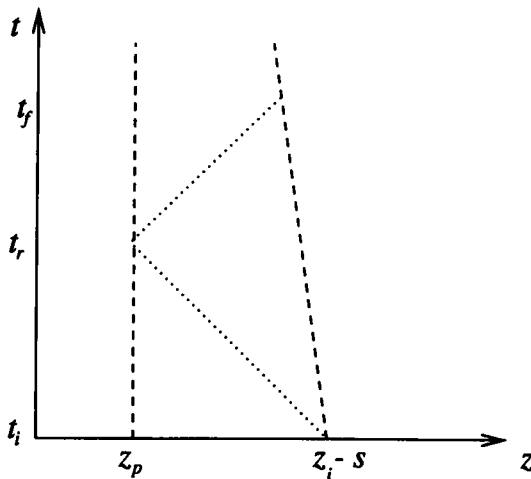


Figure 2.3: Space-time diagram showing the wave propagation (dotted lines), and the motion of the elastic-plastic interface of the projectile as seen in the rest frame of the tail.

the wave starts at the time t_i , the distance between the elastic-plastic interface and the tail is $L - s$. When the wave reflects at the tail at $t_r = t_i + \Delta t_1$, it has travelled this distance

$$c\Delta t_1 = L - s.$$

At $t_f = t_r + \Delta t_2$ the wave returns to the elastic-plastic interface. It has then travelled the return distance

$$c\Delta t_2 = L - s + \int_0^{\Delta t} (\dot{L} - \dot{s}) dt.$$

The return distance is shorter due to the effect of erosion \dot{L} and a change in the extent of the plastic zone \dot{s} . By definition the round trip time is given by $\Delta t \equiv \Delta t_1 + \Delta t_2$. Hence,

$$c\Delta t = 2(L - s) + \int_0^{\Delta t} (\dot{L} - \dot{s}) dt.$$

Taylor-expanding the integral on the right-hand-side to first order in Δt and solving for Δt , we get the first-order expression

$$\Delta t = \frac{2(L - s)}{c - u + v + \dot{s}} + \mathcal{O}(\Delta t^2) \quad (2.12)$$

where we have used the kinematical relation $\dot{L} = u - v$.

Dividing Δv Eq. (2.11) by Δt and using that $\sigma_p = Y_p$ and $E_p = \rho_p c^2$, we find

$$a_{\text{wave}} = \frac{\Delta v}{\Delta t} = -\frac{Y_p(c - u + v + \dot{s})}{c\rho_p(L - s)} + \mathcal{O}(\Delta t^2). \quad (2.13)$$

This is the deceleration of the tail induced by an elastic wave. Walker and Anderson identify $\dot{v} = \lim_{\Delta t \rightarrow 0} a_{\text{wave}}$ as the acceleration induced by a continuum of waves. Following Walker and Anderson, the equation for the tail deceleration becomes

$$\dot{v} = -\frac{Y_p(c - u + v + \dot{s})}{c\rho_p(L - s)}. \quad (2.14)$$

2.6 Equations of motion

Before writing down the equations of motion, we define the density of the projectile relative to the target density and the yield velocities of the target and the projectile by:

$$\Omega \equiv \frac{\rho_p}{\rho_t}, \quad \Upsilon_t \equiv \left(\frac{Y_t}{\rho_t}\right)^{1/2}, \quad \text{and} \quad \Upsilon_p \equiv \left(\frac{Y_p}{\rho_p}\right)^{1/2}. \quad (2.15)$$

Then, substituting the results of Eqs. (2.5), (2.7), and (2.10) into Eq. (2.3), we get

$$\begin{aligned} \dot{u} = & \left\{ \frac{2\Omega s}{2 + \varepsilon} + \frac{2\mathcal{R}(S - \mathcal{R})}{S + \mathcal{R}} \right\}^{-1} \left\{ -\frac{4\mathcal{R}^2 u^2}{(\mathcal{R} + S)^2} \dot{S} - u^2 - \frac{14}{3} \Upsilon_t^2 \log\left(\frac{S}{\mathcal{R}}\right) \right. \\ & \left. + \Omega \left[(u - v)^2 - \frac{2(u - v)}{2 + \varepsilon} \dot{s} - \frac{2[(2 + \varepsilon)L - s]\dot{v}}{2 + \varepsilon} \right] \right\} \end{aligned} \quad (2.16)$$

where s is given by Eq. (2.9). Using the yield velocity Υ_p , the equation for v becomes

$$\dot{v} = -\frac{\Upsilon_p^2}{c(L-s)}(c-u+v+\dot{s}). \quad (2.17)$$

Again, \dot{s} is found from Eq. (2.9). By pure kinematics \dot{L} and \dot{z} are given by

$$\dot{L} = u - v \quad \text{and} \quad \dot{z} = u. \quad (2.18)$$

With the assumption that of constant target plasticity radius, i.e. $\dot{S} = 0$, the system of Eqs. (2.16)–(2.18) is a complete set of equations. By substituting $d/dt \rightarrow u(z)d/dz$, and taking the variables to be function of penetration depth z instead of time t , the equations of motion can be rewritten as equations in z . This is better both from a numerical point of view and in practice, since one generally has a better intuition about penetration depths than penetration times. This is the approach taken in the *Mathematica* code [8] used in this paper.

3 APPLICATION TO CONCRETE PENETRATION

We have applied the modified Walker–Anderson model to eroding long rod penetration of concrete. Admittedly concrete is a brittle medium, and thus using a plastic material model is a bold simplification.

3.1 Model breakdown

Right after impact the projectile nose decelerates much faster than the tail. According to Equation (2.9) the projectile develops a plastic region when $v > u$. The projectile nose is decelerated by direct contact with the target and the tail is decelerated by elastic waves travelling down the projectile. For low density targets, it turns out that the Walker–Anderson model predicts that the tail is decelerated more than the nose which implies that after some time $v = u$ and $s = 0$. At this time the model breaks down. Whenever this happens, the evolution is continued using a rigid penetration model.

At this point we would like to remark that the criterium for transition to rigid penetration should be investigated further. Perhaps this transition should happen sometime before the Walker–Anderson model breaks down.

3.2 Results of numerical integration

As a test bed we have chosen the case of a projectile hitting a concrete wall. The relevant physical parameters are specified in Table 3.1. Using these data we have integrated the Walker–Anderson equations numerically.

3.2.1 Effect of smoothed velocity profile

Integration of the equations of motion for the expectation values of the input data leads to the results plotted in Figs. 3.1–3.2. The dotted curves correspond to the original

Table 3.1: *Parameters.*

Projectile		Target	
Density	17.5 g/cm ³	Density	(2.5 ± 0.05) g/cm ³
Yield limit	1.65 GPa	Target yield limit	(400. ± 40.) MPa
Initial length	16. cm	Plasticity radius	(100. ± 25.) mm
Impact velocity	1400. m/s	Crater radius	(17. ± 3.) mm
Young's modulus	165. GPa		
Sound velocity	3071. m/s		

Walker–Anderson model, and the red curves correspond to the modified model derived in this report with $\varepsilon = 1.0$.

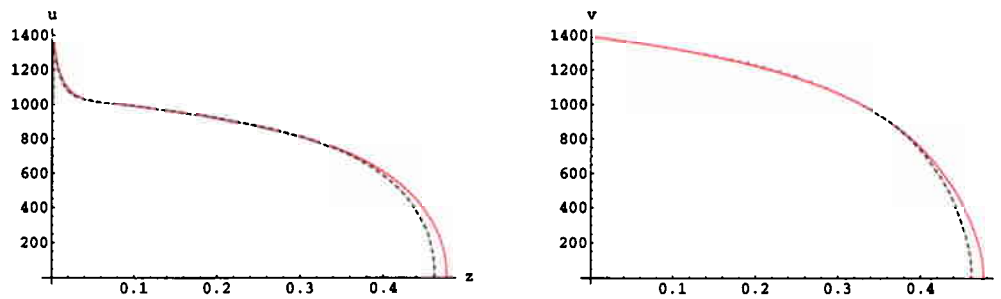


Figure 3.1: *Nose and tail velocities [m/s] as functions of depth [m]. The red curve is the new model.*

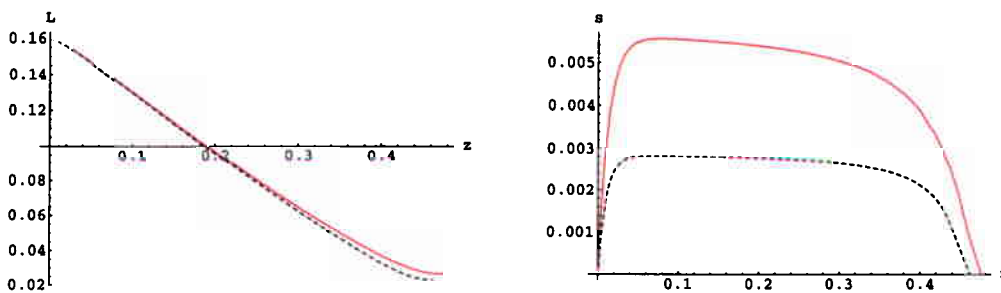


Figure 3.2: *Projectile length [m] and plasticity extension [m] as functions of penetration depth [m]. The red curve is the new model.*

The largest difference occurs for the size of the extent of plasticity in the projectile. In the new model it is up to 33% larger than in the original model. For the penetration depth and the projectile residue the changes are less than 1%. This corroborates the belief that the predictions of the Walker–Anderson model are *independent of the details of the velocity profile*. This is of course a very appealing property of the model.

carried out the integrations of the Walker–Anderson model. The resulting estimates for the cumulative distribution functions (cdf) P are shown in Fig. 3.4. The cdf is the integral of the probability density function p . Hence, it is a monotonic function P of its argument x with function values $P(x)$ spanning the interval $[0, 1]$. The value $P(a)$ is the probability that $x < a$. Look at the cdf for the penetration depth. Since $P(0.4)$ is small, there is a small probability for penetration depths smaller than 0.4 m. On the other hand, the mean value 0.493 m represents the penetration depth for which there is a fifty-fifty probability of getting a value larger or smaller. In Table 3.2 the results are given as numbers with error

Table 3.2: Penetration results.

Penetration depth	(0.493 ± 0.145) m
Projectile residue	(0.0271 ± 0.0143) m

bars corresponding to one standard deviation.

In order to find the sensitivity of penetration depth to small variations in the input parameters, we have computed the relative change in penetration depth under a small change in each of the input parameters. The resulting response in penetration depth are

Table 3.3: Responses in penetration depth and relative uncertainties of each parametre.

Parametre	response	uncertainty
Target density	42.3%	2.0%
Target yield limit	97.0%	10.0%
Extent of plasticity	52.8%	25.0%
Crater radius	59.4%	17.6%

shown in Table 3.3.

The meaning of the numbers of the response column are as follows. Suppose the target density is changed by 5%. Then the penetration depth is changed by $42.3/100 \times 5\%$. We say that the penetration depth has a 42.3% response to changes in the target density. The target yield limit is the most important parametre.

The entries in the column labelled “uncertainty” in Table 3.3 are the relative uncertainties of each input parametre. Hence, in our test case the relative uncertainty of the yield limit is much larger than that of the target density. Therefore, in this case, the most significant reduction in the prediction uncertainty can be obtained by a more precise determination of the target’s yield limit.

4 CONCLUSION

The Walker–Anderson model has been examined with a critical eye on all assumptions. An unphysical discontinuity in the first derivative of the assumed velocity field has been identified and rectified. However, in the test case studied in this paper, this discontinuity had but a negligible effect on the results.

3.2.2 Comparison with rigid penetration

It is also of interest to compare the results of the Walker–Anderson model with a pure rigid penetration model. Plots for nose and tail velocities are depicted in Fig. 3.3. Here there is a

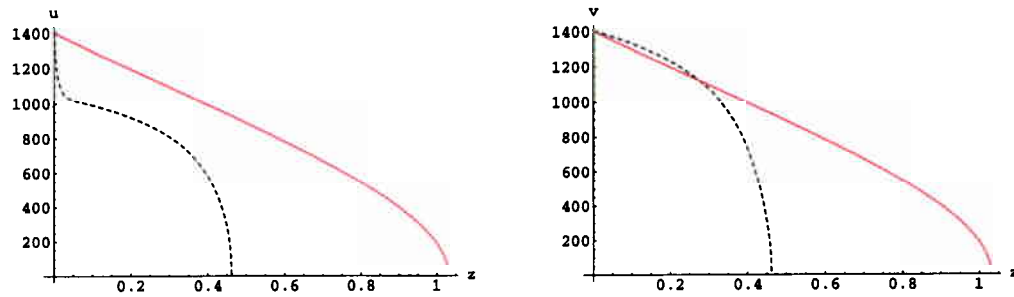


Figure 3.3: Nose and tail velocities [m/s] as functions of depth [m]. The red curve is the rigid penetration model.

striking difference between the two models. In fact, in this case the penetration depth increases almost by a factor of 2 when going from the Walker–Anderson model to a rigid penetration model.

This result should hardly come as a surprise. Yet, the importance of projectile erosion should be strongly emphasized. It plays a crucial role when computing projectile penetration depths. Making the wrong assumptions on this point have devastating consequences for the accuracy of the predictions.

3.2.3 Prediction uncertainties from parameter uncertainties

In the rest of this report we assume that the Walker–Anderson model is a good model for our penetration problem.

Even when the modelling framework is fixed there are uncertainties in many material parameters.

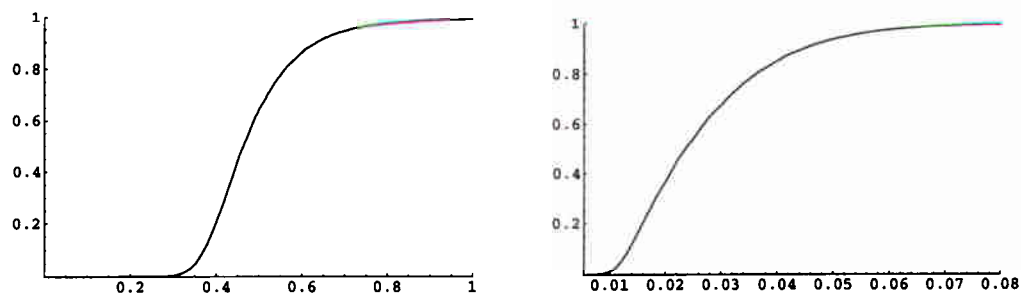


Figure 3.4: Plots of the estimated cumulative distribution functions (cdf's) for the penetration depth [m] and projectile residues [m].

Assuming that the target parameters have normally distributed uncertainties, we have run 10000 simulations where we have drawn material properties from these distributions and

The effect of uncertainties in the input parameters has been studied and (in the test case) the largest contribution has been found to be the target's yield limit. As mentioned in Section 2.4 the simplistic modelling of the yield limit leaves room for improvement of the model. One step in this direction has been taken by Walker and Anderson who have generalized their model to include the Drucker–Prager constitutive model [7].

Within the framework of the Walker–Anderson model or any other semi-analytical model, it is possible to perform a large number of numerical integrations and thus to draw enough samples from the input data distributions to give reliable estimates of the prediction uncertainties. For most practical purposes knowledge about the uncertainty of a prediction is almost as important as the prediction itself. In this report we have carried out such a statistical analysis based on 10000 simulations with stochastic input parameters.

However, it should be stressed that more work is needed both theoretically and experimentally before these methods can be made sufficiently reliable to be used as a design tool. In particular, one ought to work out a better criterium for transition to rigid penetration. In the present work a breakdown of the Walker–Anderson model signals this transition. We also think that the model merits a better experimental backing. Hence, it would be valuable to have a large data set with penetration results for a variety of targets and penetrators with careful measurements of material data with estimates of the uncertainties of all available data.

ACKNOWLEDGEMENT

The authors are grateful to J. A. Teland for his critical reading of the manuscript and for helpful comments.

APPENDIX

A NOTATION

E_p	Youngs's modulus of projectile
L	projectile length
\mathcal{O}	order of
\mathcal{R}	crater radius
S	radius of plastic flow in target
Y_p	projectile yield limit
Y_t	target yield limit
Y_0	yield limit at zero pressure
\bar{Y}	yield limit on plateau
a_{wave}	wave induced acceleration
c	speed of sound in projectile
r	spherical radius
s	extent of plastic flow in projectile
t	time
t_i	starting time of elastic wave
t_r	reflection time of elastic wave
t_f	return time of wave
u	interface (penetration) velocity
u_k	velocity component in k -direction
v	projectile (tail) velocity
z	axial coordinate
z_i	axial position of projectile/target interface (nose position)
z_{i-}	left limit of nose position
z_{i+}	right limit of nose position
z_p	axial position of projectile tail
Δt	wave round-trip travelling time
Δt_1	wave travelling time to reflection
Δt_2	wave return trip travelling time
Υ_p	yield velocity of projectile
Υ_t	yield velocity of target
Ω	relative density ρ_p/ρ_t
ε	dimensionless shape parametre for the velocity profile
ρ	density
ρ_p	projectile density
ρ_t	target density
σ_p	projectile flow stress
σ_{ij}	stress tensor
∂_y	partial derivative operator $\partial/\partial y$
$A_{x,y}$	partial derivative: $\partial_y A_x \equiv \partial A_x / \partial y$
\dot{A}	time derivative of A

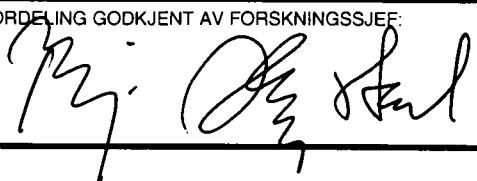

References

- [1] Alekseevskii V P (1966): Penetration of a rod into a target at high velocity, *Combustion, Explosion and Shock Waves* (translated from Fizika Goreniya i Vrzhyva) **2**, 63–66.
- [2] Tate A (1967): A theory for the deceleration of a rod into a target at high velocity, *J. Mech. Phys. Solids* **15**, 387–399.
- [3] Tate A (1969): Further results in the theory of long rod penetration, *J. Mech. Phys. Solids* **17**, 141–150.
- [4] Teland J A (1999): A Review of Analytical Penetration Mechanics, FFI/RAPPORT-99/01264, Forsvarets Forskningsinstitut (Norwegian Defence Research Establishment), P.O. Box 25, NO-2027 Kjeller, Norway.
- [5] Birkhoff G, MacDougall D P, Pugh E M, Taylor G (1948): Explosives with lined cavities, *J. Applied. Phys.* **19**, 6, 563–582.
- [6] Walker J D, Anderson Jr. C E (1995): A time-dependent model for long-rod penetration, *Int. J. Impact Engng.* **16**, 1, 19–48.
- [7] Walker J D, Anderson Jr. C E (1998): Penetration modelling of ceramic and metal targets, In: *36th Aerospace Sciences Meeting & Exhibit: January 12–15, 1998/Reno, NV*, AIAA 98-0829, American Institute of Aeronautics and Astronautics, 1801 Alexander Bell Drive, Suite 500, Reston, Virginia 20191-4344, USA.
- [8] Soleng H H (2000): Penetration.m version 1.0: a Mathematica implementation of an analytical penetration model, FFI/RAPPORT-2000/05875, Forsvarets Forskningsinstitut (Norwegian Defence Research Establishment), P.O. Box 25, NO-2027 Kjeller, Norway.

DISTRIBUTION LIST

FFIBM

Dato: 15 januar 2001

RAPPORTTYPE (KRYSS AV) <input checked="" type="checkbox"/> RAPP <input type="checkbox"/> NOTAT <input type="checkbox"/> RR		RAPPORT NR. 2000/05876	REFERANSE FFIBM/766/130	RAPPORTENS DATO 15 januar 2001
RAPPORTENS BESKYTTELSESGRAD Unclassified		ANTALL EKS UTSTEDT 46	ANTALL SIDER 21	
RAPPORTENS TITTEL PENETRATION MODELLING WITH UNCERTAINTY QUANTIFICATION USING THE WALKER-ANDERSON MODEL		FORFATTER(E) SOLENG Harald H, SVINSÅS Eirik		
FORDELING GODKJENT AV FORSKNINGSSJEF: 		FORDELING GODKJENT AV AVDELINGSSJEF: 		

EKSTERN FORDELING

INTERN FORDELING

ANTALL	EKS NR	TIL	ANTALL	EKS NR	TIL
1		FBT/S	14		FFI-Bibl
1		Helge Langberg	1		Adm direktør/stabssjef
1		FOA	1		FFIE
1		Håkan Hansson	1		FFISYS
1		Mattias Unosson	5		FFIBM
		SE-14725 Tumba, Sverige	1		FFIN
1		TNO	1		Bjarne Haugstad, FFIBM
1		Jaap Weerheijm	1		Eirik Svinsås, FFIBM
1		Cyril Wentzel	1		Harald H Soleng, FFIBM
		Lange Kleinweg 137	1		Jan Arild Teland, FFIBM
		PO Box 45	1		Henrik Sjøel, FFIBM
		NL-2280 AA RIJSWIJK, Nederland	1		John F Moxnes, FFIBM
1		DERA	1		Ove Dullum, FFIBM
1		Cathy O'Carroll	1		Svein E Martinussen, FFIBM
1		Jim Sheridan			FFI-veven
		X107, Barnes Wallis Building			
		Farnborough			
		Hampshire GU14OLX			
		UK			
1		EMI			
1		Werner Riedel			
		Ecker Strasse 4			
		79104 Freiburg			
		Germany			

FFI-K1

Retningslinjer for fordeling og forsendelse er gitt i Oraklet, Bind I, Bestemmelser om publikasjoner for Forsvarets forskningsinstitutt, pkt 2 og 5. Benytt ny side om nødvendig.